



UNIVERSITY OF LEEDS

This is a repository copy of *Modulation of microsaccades by spatial frequency during object categorization..*

White Rose Research Online URL for this paper:
<http://eprints.whiterose.ac.uk/108527/>

Version: Accepted Version

Article:

Craddock, M, Oppermann, F, Müller, MM et al. (1 more author) (2017) Modulation of microsaccades by spatial frequency during object categorization. *Vision Research*, 130. pp. 48-56. ISSN 0042-6989

<https://doi.org/10.1016/j.visres.2016.10.011>

© 2016 Elsevier Ltd. Licensed under the Creative Commons Attribution-NonCommercial-NoDerivatives 4.0 International
<http://creativecommons.org/licenses/by-nc-nd/4.0/>

Reuse

Unless indicated otherwise, fulltext items are protected by copyright with all rights reserved. The copyright exception in section 29 of the Copyright, Designs and Patents Act 1988 allows the making of a single copy solely for the purpose of non-commercial research or private study within the limits of fair dealing. The publisher or other rights-holder may allow further reproduction and re-use of this version - refer to the White Rose Research Online record for this item. Where records identify the publisher as the copyright holder, users can verify any specific terms of use on the publisher's website.

Takedown

If you consider content in White Rose Research Online to be in breach of UK law, please notify us by emailing eprints@whiterose.ac.uk including the URL of the record and the reason for the withdrawal request.



eprints@whiterose.ac.uk
<https://eprints.whiterose.ac.uk/>

21 Abstract

22

23 The organization of visual processing into a coarse-to-fine information processing based on
24 the spatial frequency properties of the input forms an important facet of the object recognition
25 process. During visual object categorization tasks, microsaccades occur frequently. One
26 potential functional role of these eye movements is to resolve high spatial frequency
27 information. To assess this hypothesis, we examined the rate, amplitude and speed of
28 microsaccades in an object categorization task in which participants viewed object and non-
29 object images and classified them as showing either natural objects, man-made objects or
30 non-objects. Images were presented unfiltered (broadband; BB) or filtered to contain only
31 low (LSF) or high spatial frequency (HSF) information. This allowed us to examine whether
32 microsaccades were modulated independently by the presence of a high-level feature – the
33 presence of an object – and by low-level stimulus characteristics – spatial frequency. We
34 found a bimodal distribution of saccades based on their amplitude, with a split between
35 smaller and larger microsaccades at 0.4° of visual angle. The rate of larger saccades ($\geq 0.4^\circ$)
36 was higher for objects than non-objects, and higher for objects with high spatial frequency
37 content (HSF and BB objects) than for LSF objects. No effects were observed for smaller
38 microsaccades ($< 0.4^\circ$). This is consistent with a role for larger microsaccades in resolving
39 HSF information for object identification, and previous evidence that more microsaccades are
40 directed towards informative image regions.

41

42 Keywords: microsaccades, eye movements, object categorisation, object identification,
43 spatial frequency

44

1. Introduction

45
46 Object recognition is based on a cascade of feedforward and feedback mechanisms through
47 the visual processing hierarchy (e.g. Bar et al., 2006; Hochstein & Ahissar, 2002; VanRullen,
48 2007). This cascade may follow a coarse-to-fine sequence in which spatial frequency
49 information may be particularly important for coding information at different spatial and
50 temporal scales (e.g. Bullier, 2001; Goffaux et al., 2010; Hegdé, 2008; Kauffmann,
51 Ramanoel, & Peyrin, 2014). Initial, feedforward processing may rely on low spatial
52 frequencies (LSF), which provide information about many features of the visual input in
53 parallel, activating compatible nodes in a recognition network (e.g. Levin, Takarae, Miner, &
54 Keil, 2001). However, the conscious identification of objects likely requires re-entrant
55 processing (feedback mechanisms) with focused attention onto the location of decisive
56 features of potential objects (e.g. Di Lollo, Enns, & Rensink, 2000; Evans & Treisman, 2005;
57 Hochstein & Ahissar, 2002). High spatial frequency (HSF) information may provide more
58 fine-grained details and boundaries necessary for object identification (e.g. Oliva & Schyns,
59 1997; Oliva & Torralba, 2006). While a single glance may rapidly capture LSFs in a visual
60 scene, resolving HSFs and fine spatial detail may require microsaccades (Ko, Poletti, &
61 Rucci, 2010; McCamy, Otero-Millan, Stasi, Macknik, & Martinez-Conde, 2014; Otero-
62 Millan, Troncoso, Macknik, Serrano-Pedraza, & Martinez-Conde, 2008; Rucci, 2008; Rucci,
63 Iovin, Poletti, & Santini, 2007; Turatto, Valsecchi, Tamè, & Betta, 2007). Microsaccades are
64 small eye movements – typically up to 1° of visual angle – that occur frequently even during
65 fixation (for reviews, see Martinez-Conde, Macknik, Troncoso, & Hubel, 2009; Martinez-
66 Conde, Otero-Millan, & Macknik, 2013; Melloni, Schwiedrzik, Rodriguez, & Singer, 2009;
67 Rolfs, 2009). The present study investigates how the occurrence of microsaccades depends on
68 the spatial frequency and object information of the visual input.

69 Spatial frequency information at different scales contributes to object categorization
70 in different ways. LSFs may be processed and reach higher-order areas faster than HSFs (Bar
71 et al., 2006). LSFs provide coarse global image features associated with the rough shape and
72 layout of objects, helping to determine, for example, scene category. Scene category can be
73 extracted at the first glance as reflected in differential cerebral activity after 150 ms, even
74 with visual exposures starting from 20 ms (Fabre-Thorpe, Richard, & Thorpe, 1998; Thorpe,
75 Fize, & Marlot, 1996; VanRullen & Thorpe, 2001). This processing occurs without directly
76 attending the target image and might thus rely on the first feedforward sweep of activation
77 (Li, VanRullen, Koch, & Perona, 2002; Rousselet, Fabre-Thorpe, & Thorpe, 2002; Thorpe,
78 Gegenfurtner, Fabre-Thorpe, & Bülthoff, 2001). LSF processing may form a major part of
79 this initial feedforward sweep (Bullier, 2001).

80 When comparing pictures of objects filtered for spatial frequency content, intact
81 unfiltered pictures as well as pictures containing both LSF and HSF information showed
82 better performance compared with pictures only containing either LSF or HSF information
83 from around 100 ms of exposure duration (Kihara & Takeda, 2010, 2012). Importantly, the
84 categorization of LSF-only objects outperformed the categorization of HSF objects for the
85 exposure durations of up to 250 ms, suggesting a prior for LSF information in early
86 processing in this kind of categorization task (Kihara & Takeda, 2010). The differences did
87 not change when attentional demands were increased, suggesting that the effects are based on
88 the first feedforward processing (Kihara & Takeda, 2012).

89 However, the information extracted during feedforward processing does not always
90 allow full, accurate identification of scenes and objects within them. For example, Evans and
91 Treisman (2005) asked their participants to identify animal targets embedded in RSVP
92 streams of distractors, with each image presented for 75-100 ms. The participants failed to
93 identify the targets in more than half of the trials, and also often failed to localize the target

94 correctly, suggesting that further processing is necessary. After the feedforward sweep comes
95 re-entrant, feedback processing, which is likely directed at processing of HSFs. For example,
96 consistent with the expectation that processing of HSF information follows processing of
97 LSF information, coarse-to-fine, LSF-to-HSF image sequences of scenes elicit greater earlier
98 activation in early occipital areas and both frontal and temporal areas compared to fine-to-
99 coarse HSF-to-LSF sequences (Peyrin et al., 2010).

100 Eye movements in this period may be particularly important. Microsaccades follow a
101 stereotypical pattern of inhibition and subsequent release after the onset of a visual stimulus,
102 dropping significantly before rebounding to a new peak after approximately 200-400 ms (e.g.
103 Engbert & Kliegl, 2003; Turatto et al., 2007). They are affected by a range of cognitive
104 factors such as task difficulty and attention (Engbert, 2006; Engbert & Kliegl, 2003;
105 Siegenthaler et al., 2014), and change neural processing (Bosman, Womelsdorf, Desimone, &
106 Fries, 2009; Dimigen, Valsecchi, Sommer, & Kliegl, 2009; Martinez-Conde, Macknik, &
107 Hubel, 2000, 2002; Troncoso et al., 2015). The amplitudes of saccades in these studies range
108 from less than 1° of visual angle, which are typically defined as microsaccades (Martinez-
109 Conde et al., 2013; Melloni et al., 2009), up to 1.5° or 2.0° (e.g. Engbert & Kliegl, 2003;
110 Martinez-Conde, Macknik, Troncoso, & Dyar, 2006; Turatto et al., 2007; Yuval-Greenberg,
111 Tomer, Keren, Nelken, & Deouell, 2008). Stimulus and fixation target size may also
112 influence microsaccade amplitude ((McCamy, Najafian Jazi, Otero-Millan, Macknik, &
113 Martinez-Conde, 2013; Otero-Millan, Macknik, Langston, & Martinez-Conde, 2013).

114 With regard to spatial frequency, there is evidence to suggest that HSF may increase
115 the rate of microsaccades. Microsaccades occur at a higher rate during tasks which require
116 high visual acuity (Ko et al., 2010), show directional biases during tasks that involve
117 discrimination of visual detail (Turatto et al., 2007), and occur more frequently during
118 foveation of faces or other salient objects (Otero-Millan et al., 2008). They also occur more

119 frequently in more informative regions of visual scenes, such as those with high contrast and
120 low spatial correlation (McCamy et al., 2014). Bonneh, Adini, & Polat (2015) tested
121 microsaccade rates in response to passive viewing of transient Gabor patches with varying
122 spatial frequency. They found that microsaccade latency following release from inhibition
123 increased as spatial frequencies went from middle-level (2 cycles per degree) to higher (8
124 cycles per degree), which may have produced a later, smaller peak in microsaccade rate.
125 However, microsaccade rates in passive viewing tasks may not reflect performance in more
126 directed, active viewing tasks (e.g. McCamy et al., 2014).

127 Consistent with a role of microsaccades in object recognition, it has been
128 demonstrated that the rebound peak in the saccade rate after the onset of a visual stimulus is
129 modulated by high-level stimulus properties; for example, it is relatively elevated for objects
130 compared to non-object stimuli (Hassler, Barreto, & Gruber, 2011; Keren, Yuval-Greenberg,
131 & Deouell, 2010; Yuval-Greenberg et al., 2008). However, this evidence comes primarily
132 from investigations of the relationship between microsaccades and a broadband peak in
133 induced gamma band oscillations (~30-100 Hz), observed using the scalp-recorded
134 electroencephalogram (EEG). This signal was considered to be a signature of the activation
135 of an object representation and the binding of the activity of disparate populations of neurons,
136 each representing distinct object features, into a single coherent percept (Tallon-Baudry &
137 Bertrand, 1999). Several authors have convincingly demonstrated that an electrical, muscle-
138 generated signal associated with microsaccades – the saccade spike potential (SSP) –
139 underlies this effect (Hassler et al., 2011; Keren et al., 2010; Yuval-Greenberg et al., 2008).
140 Thus, many of the reported modulations of induced gamma-band activity – for example, by
141 object orientation (Martinovic, Gruber, & Müller, 2007, 2008) – were likely attributable to
142 modulations of the underlying saccade rate in the critical window around 200-400 ms.
143 Directly examining the saccade rate in this time window may thus reveal information

144 regarding object recognition processes and role of eye-movements to resolve spatial
145 frequency information.

146 In the present study, we use a living/non-living categorization task to probe the role of
147 spatial frequency in object processing by varying the spatial frequency content of objects. We
148 presented objects either as unfiltered, broadband (BB) images, or filtered to contain only LSF
149 or HSF content. We chose spatial frequency ranges that corresponded to previous studies
150 examining the different roles of HSF and LSF in object recognition (e.g. Bar et al., 2006).
151 These ranges also correspond to the spatial frequency tuning curves observed in orbitofrontal
152 and visual cortices (Fintzi & Mahon, 2013). We expected that we would observe the typical
153 peaks in the saccade rate approximately 200-400 ms after stimulus onset. Given that
154 microsaccades may have a role in resolving fine spatial detail, we expected to see higher rates
155 for HSF and BB images than for images with LSF only. Additionally, we presented non-
156 object trials with spatial frequency content matched to that of the object images. We expected
157 that saccade peak rates would be reduced relative to object trials, in line with previous
158 findings from EEG (e.g. Hassler et al., 2011; Yuval-Greenberg et al., 2008), and in free-
159 viewing of blank scenes (Otero-Millan et al., 2013, 2008). Nevertheless, object versus non-
160 object differences should also reveal whether differences in saccade rate are driven by high-
161 level factors in combination with low-level stimulus properties, or low-level stimulus
162 properties alone: spatial frequency differences on non-object trials would imply the latter. To
163 better characterise the saccades, we also examined their latency, amplitude and peak velocity.

164

165

2. Method

2.1 Participants

167 Twelve participants were recruited; all students from the University of Leipzig (ages 20 to
168 28; mean = 24). 7 were female, 5 male. All participants reported normal vision. Participants

169 received course credit for their participation. The study was conducted in line with the
170 requirements of the local ethics committee of the University of Leipzig, and written informed
171 consent was taken in accordance with the Code of Ethics of the World Medical Association
172 (Declaration of Helsinki).

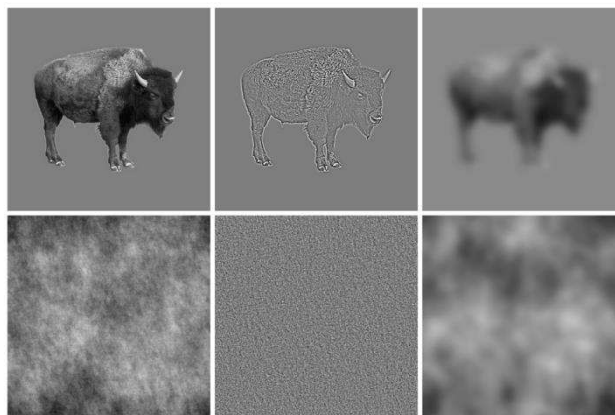
173

174 **2.2 Stimuli and apparatus**

175 We selected a set of 240 greyscale photographs from a commercial image database (Hemera
176 Photo Objects), which comprised 120 photographs depicting natural objects (e.g. animals,
177 fruit) and 120 showing man-made objects (e.g. furniture, tools). Only photographs showing a
178 single object in isolation were selected. HSF and LSF versions of each object were produced
179 from the unfiltered, broadband images (BB) by multiplying the Fourier energy of the fast
180 Fourier transform of each BB image with a Gaussian filter that either attenuated spatial
181 frequencies below ~ 4.7 cycles per degree (cpd) for HSF images or above ~ 0.9 cpd for LSF
182 images. These settings were comparable to the filtering used by Bar et al. (2006), and also
183 reflect the sensitivities of the visual and orbitofrontal cortices (Fintzi & Mahon, 2013). For
184 each BB, HSF, and LSF image, a matching non-object was created by producing a noise
185 texture with the same amplitude spectrum and spatial frequency content as the original image.
186 This was achieved by randomising the phase of the object image's Fourier transformation.
187 The mean (global luminance) and standard deviation (RMS contrast) of every BB, HSF, and
188 LSF image was adjusted to match the mean global luminance and RMS contrast of the full set
189 of BB images (see Figure 1).

190 Visual stimuli were presented centrally on a 19-in Eizo FlexScan S1910 monitor at a
191 screen resolution of 1280×1024 pixels, and seen from a viewing distance of 80 cm. Stimulus
192 size (including a grey background) was 400×400 pixels. The stimuli subtended
193 approximately 10 degrees of visual angle in each direction.

194 Eye movements were recorded at 500 Hz using the EyeLink II (SR Research Ltd.,
195 ON, CA). Motions of the participant's head were restrained by using a head rest. Stimulus
196 presentation and data recordings were controlled by the SR Research Experiment Builder
197 software.



198
199 **Figure 1** Sample stimuli. Columns show unfiltered, high-pass filtered, and low-pass
200 filtered images. Noise images in the lower row were created by randomising the phase
201 of the FFT of the intact object. All pictures were matched for global luminance and
202 RMS contrast.

203

204 2.3 Design

205 The experiment comprised a two factor design with six different conditions: object (object or
206 non-object noise texture) \times spatial frequency (BB, HSF, LSF). There were 480 trials split
207 across six blocks of 80 trials. The order of trials was randomised for each participant. On half
208 of the trials, participants saw a BB, HSF, or LSF object. Half of these objects were natural,
209 half man-made. On the other half of trials, participants saw a BB, HSF, or LSF non-object
210 texture. The objects presented in each condition were counterbalanced across participants.
211 Thus, each participant saw each object in only one spatial frequency condition, but each
212 object was presented an equal number of times in every condition over the course of the
213 experiment.

214 Each trial began with a white fixation cross on a black background presented for a
215 variable period of 500-800 ms. A stimulus image was then presented for 500 ms. Then, the
216 fixation cross reappeared and remained on screen for 1000 ms, after which the screen was
217 blanked for a variable period of 900-1200 ms. Participants were encouraged to use this time
218 to blink if they needed to do so. Participants pressed a different button to indicate the
219 category to which each image belonged: natural object, man-made object, or non-object
220 texture. Note that we subsequently collapsed responses across man-made and natural objects,
221 since our primary interest was in the contrast between objects and non-objects. Participants
222 first performed a practice block of 54 trials, which presented a set of practice images created
223 in the same manner as the experimental images but were not shown during the main
224 experiment. Participants were asked to minimize blinking and eye movements while a
225 stimulus or fixation cross was displayed, and to respond as quickly as possible while aiming
226 to minimize errors.

227

228 **2.4 Behavioural data analysis**

229 Only RTs on correct trials were included in the analysis (3.7% of the data were coded as
230 errors). RTs were considered as outliers and excluded from the analysis when they deviated
231 more than 2.5 standard deviations from the subject's mean in a respective condition (further
232 1.7% of the data). Reaction times (RTs) and errors were then analysed using a two-way
233 repeated-measures analysis of variance (ANOVA) with the factors Object (Object versus
234 Non-object) and Frequency (BB, HSF, or LSF). Generalized eta squared is reported to
235 estimate the effect size. If required, post-hoc t-tests were conducted with Bonferroni-Holm
236 correction for multiple comparisons.

237

238 **2.5 Eye-tracking analysis**

239 A time window from 500 ms before to 700 ms after picture onset was selected for analysis.
240 Trials were discarded from the analyses if either (a) a blink was within the analyzed time
241 window, or (b) position data from either of the eyes were missed in the relevant time window.
242 We excluded 4.4% of the data from the analysis. Microsaccades were detected using the
243 Engbert and Mergenthaler procedure (2006; see also Engbert & Kliegl, 2003). This algorithm
244 is based on eye movement velocity, with horizontal and vertical velocities computed
245 separately. The detection threshold was calculated relative to noise as $\lambda = 6$ multiples of the
246 median-based SD. Saccades were determined for each eye separately, but only binocular
247 events with a minimal temporal overlap of 6 ms were accepted. To control for overshoot
248 components, which can result from corrections of fixations after saccades, only saccades
249 which occurred at least 30 ms after the previous saccade were considered as microsaccades
250 (see also Mergenthaler & Engbert, 2010). The saccade rate reflects the estimated number of
251 saccades in a trial per second. The saccade rate was determined in bins of 20 ms. Data were
252 analysed using the same two-way repeated-measures ANOVA as the behavioural data
253 consisting of the factors Object and Frequency.

254 3. Results

255 3.1 Behavioural data

256 Participants responded slower [$F(1, 11) = 61.98, p < .001, \eta_g^2 = .28$] and made more errors
257 [$F(1,11) = 6.00, p = .03, \eta_g^2 = .11$] when responding on object (732 ms; 6.9% errors) than non-
258 object trials (580 ms; 0.4%).

259 There were significant main effects of Frequency for RTs [$F(2, 22) = 43.76, p < .001,$
260 $\eta_g^2 = .03$] and errors [$F(2,22) = 5.78, p < .01, \eta_g^2 = .12$] with comparable reaction times and
261 error rates to BB (642 ms, 1.3 % errors) and HSF images (637 ms; 1.1%), and slower and less
262 accurate responses to LSF images (688 ms; 8.6%).

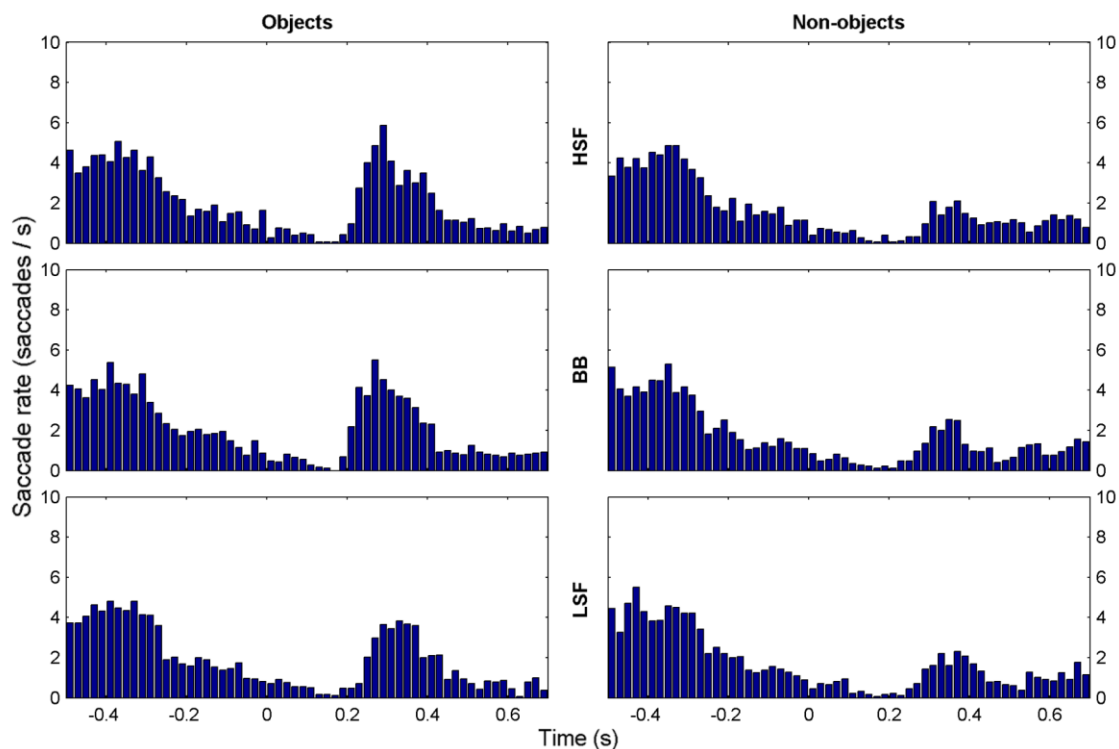
263 Most important, the interaction between Object and Frequency was also significant
 264 for RTs [$F(2, 22) = 21.19, p < .001, \eta_g^2 = .02$] and errors [$F(2,22) = 5.32, p = .01, \eta_g^2 = .11$].
 265 Post-hoc tests (p-value adjusted) revealed that RTs on objects were significantly slower than
 266 on non-objects (BB, HSF, and LSF; all $p_s < .001$). Additionally, responses to LSF objects
 267 (RT: $M = 784$ ms, $SE = 8$ ms; error: $M = 16.7\%$, $SE = 23.5\%$) were slower and more error-
 268 prone than responses to both BB (RT: $M = 701$ ms, $SE = 10$ ms, $t(11) = 6.48, p < .001$; error:
 269 $M = 2.2\%$, $SE = 2.8\%$, $t(11) = 2.31, p < .05$) and HSF objects (RT: $M = 711$ ms, $SE = 9$ ms,
 270 $t(11) = 7.56, p < .001$; error: $M = 1.9\%$, $SE = 2.7\%$, $t(11) = 2.42, p < .05$), while no
 271 difference was observed between BB and HSF objects (RT: $t(11) = 1.41, p = .37$; errors: $t < 1$).
 272 Furthermore, responses on HSF non-objects (RT: $M = 564$ ms, $SE = 12$ ms) were faster than
 273 responses on BB (RT: $M = 583$ ms, $SE = 13$ ms; $t(11) = 4.59, p < .01$) and LSF non-objects
 274 (RT: $M = 592$ ms, $SE = 12$ ms; $t(11) = 4.35, p < .01$), while no difference was observed
 275 between BB and LSF non-objects ($t(11) = 1.34, p = .37$). There were no differences in error
 276 rates between non-object trials (BB: $M = 0.4\%$, $SE = 0.6\%$, HSF: $M = 0.3\%$, $SE = 0.6\%$,
 277 LSF: $M = 0.5\%$, $SE = 0.8\%$; $t_s < 1$).

278

279 **3.2 Eye movement data**

280 To determine whether overall saccade rate changes after stimulus presentation, we compared
 281 saccade rates averaged across all conditions in three time-windows (baseline: -200-0 ms,
 282 poststimulus I: 0-200 ms, and poststimulus II: 200-400 ms). Figure 2 shows the microsaccade
 283 rate for each condition averaged across participants. Note that saccade rate is increased before
 284 the baseline window. These saccades are likely to reflect movements to re-fixate the fixation
 285 cross, which appeared 500 to 800 ms before stimulus onset following a blank screen during
 286 which participants was allowed to blink. The saccade rate (baseline: $M = 1.43$ saccades/s; SE
 287 $= .19$) decreased after stimulus presentation (poststimulus I: $M = .43$ saccades/s; $SE = .10$; t -

288 test: $t(11) = 9.26, p < .001$) before increasing relative to the baseline in the later time window
 289 (poststimulus II: $M = 2.28$ saccades/s; $SE = .26$; t-test: $t(11) = 5.11, p < .001$).



290

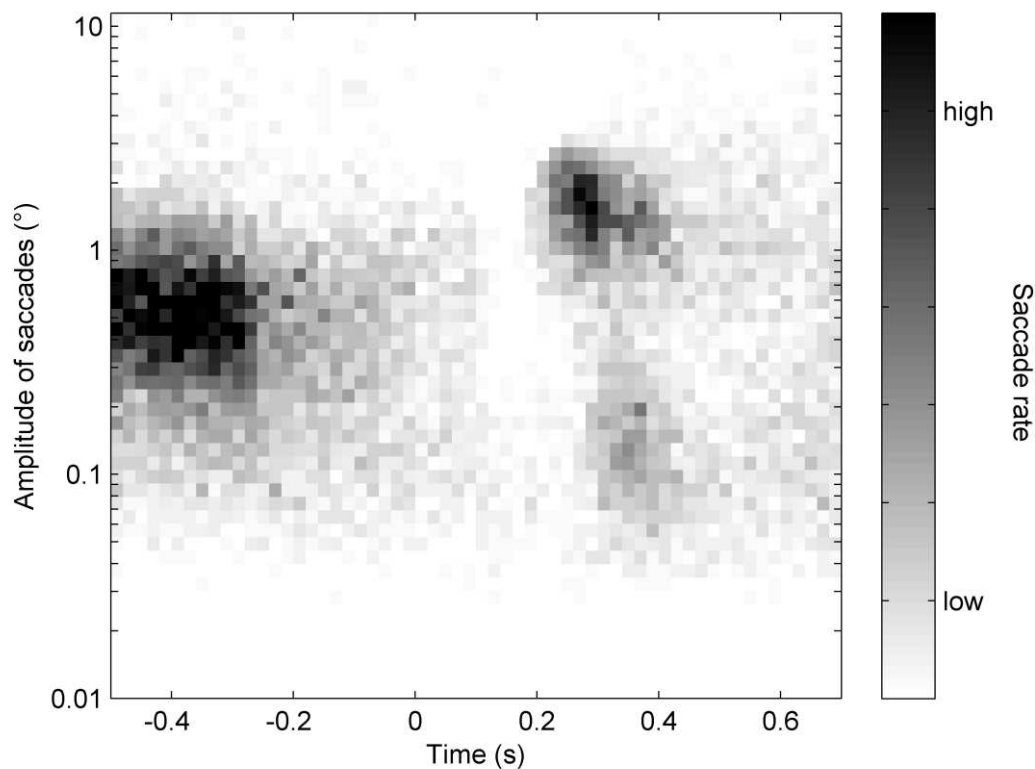
291 **Figure 2** Group ($N = 12$) mean rate of detected eye movements in the eye-tracking
 292 experiment over time (bin width = 20 ms), separated by condition. Left column shows
 293 eye movements on trials in which objects were present; right column shows movements
 294 on trials in which non-objects were presented. From top to bottom, the rows show
 295 events when high spatial frequency (HSF), broadband (BB), and low spatial frequency
 296 (LSF) images were presented. Note the higher rate of microsaccades in the object
 297 conditions from 200-400 ms.

298

299 Before comparing saccade rates between conditions, we examined saccade amplitudes.

300 Figure 3 shows the distribution of amplitudes over time averaged across all conditions, with
 301 shades of gray reflecting the saccade rate. Overall, saccade amplitudes were mostly between
 302 0.05° and 3° of visual angle. The smallest saccade that we detected with the procedure was
 303 0.03° , which reflects the technical limit of the video-based eye-tracker to measure saccades.

304 The initial drop in saccade rate after stimulus presentation is clearly visible, with a
 305 subsequent increase around 200-400 ms after stimulus presentation. However, as the saccade
 306 rate changed over time, the distribution of saccades of different amplitudes also changed.
 307 Most interestingly, the saccades in the 200-400 ms time window follow a bimodal amplitude
 308 distribution. Smaller saccades peak at a mean amplitude of 0.12° , whereas larger saccades
 309 peak around 1.36° . To rule out that this bimodal distribution is driven by a couple of subjects
 310 only, we looked at plots of individual subject data (see Supplementary Figure 1). A clear
 311 bimodality can be observed for the majority of subjects. Figure 3 also suggests that there may
 312 be a latency difference between larger ($M=317\text{ms}$, $SD=24\text{ms}$) and smaller saccades
 313 ($M=328\text{ms}$, $SD=35\text{ms}$), but this is not significant ($t(11)<1$, $p=.39$).



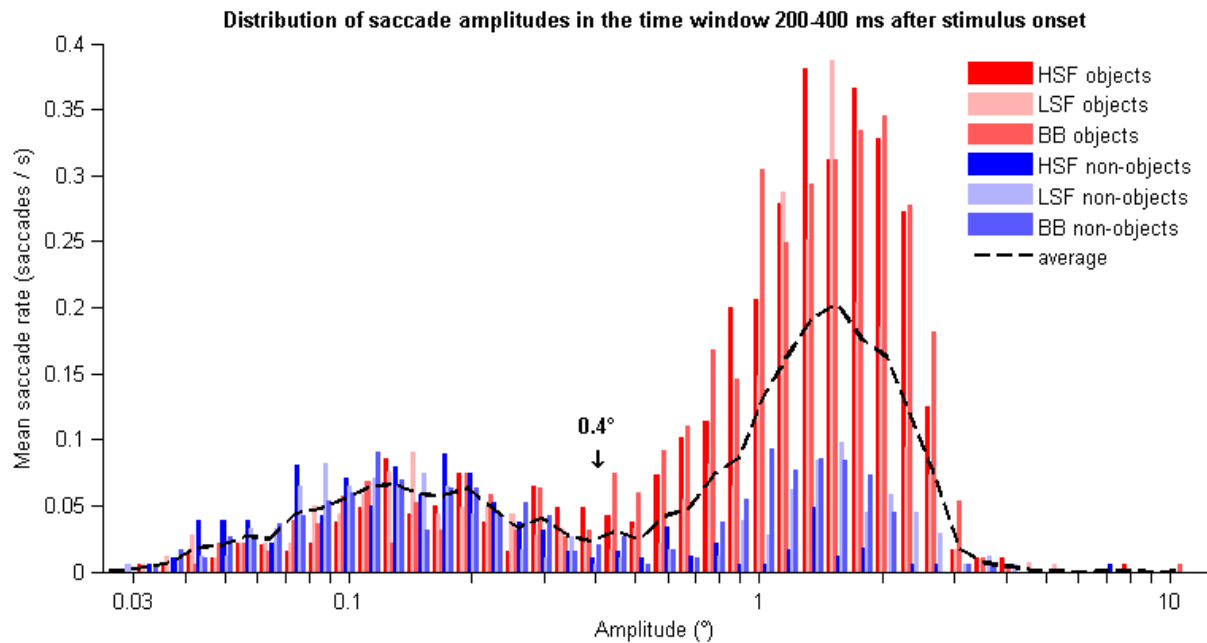
314
 315 **Figure 3** Distribution of saccade amplitudes over time (pooled across subjects ($N = 12$)
 316 and conditions; bins of 20 ms and a log amplitude of 0.06). Amplitude axis is plotted on
 317 a logarithmic scale. Note the presence of a bimodal distribution after the initial

318 inhibitory decrease in rate compared to the unimodal distribution in the pre-stimulus
319 window

320

321 For further analyses, we focused on the critical time window from 200-400 ms after
322 stimulus onset. Figure 4 shows the clear bimodal distribution of saccade amplitudes in this
323 time window for each condition. While the distribution of the microsaccades seems to be
324 comparable between conditions, the saccade rate differs clearly between conditions for larger
325 saccades. The rate of the larger saccades is higher when objects (bluish bars) rather than non-
326 objects (reddish bars) were presented. We analyzed the saccades around these two distinct
327 peaks of amplitudes separately. The trough between the peaks was used as the boundary with
328 saccades smaller than 0.4° as small microsaccades and saccades larger or equal to 0.4° as
329 large microsaccades (see also Mergenthaler & Engbert, 2010). There are single saccades with
330 amplitudes clearly outside of the two distributions. These outliers were excluded from further
331 analyses of the two saccade types. Saccades were considered as outliers when their amplitude
332 deviated from the participant's mean of the respective conditions more than 2.5 standard
333 deviations. According to this criterion, 4 saccades (0.5 %) were excluded from the analysis of
334 small microsaccades and 24 (1.4 %) from the analysis of large microsaccades. Small
335 microsaccades considered for analysis showed a mean amplitude of 0.12° of visual angle
336 ($SD = 1.32^\circ$). Large microsaccades showed a mean amplitude of 1.27° of visual angle ($SD =$
337 1.30°).

338



339

340 **Figure 4** Distribution of saccade amplitudes in the time window from 200-400 ms after
 341 stimulus onset averaged across subjects (N = 12; bins with a log amplitude of 0.06).

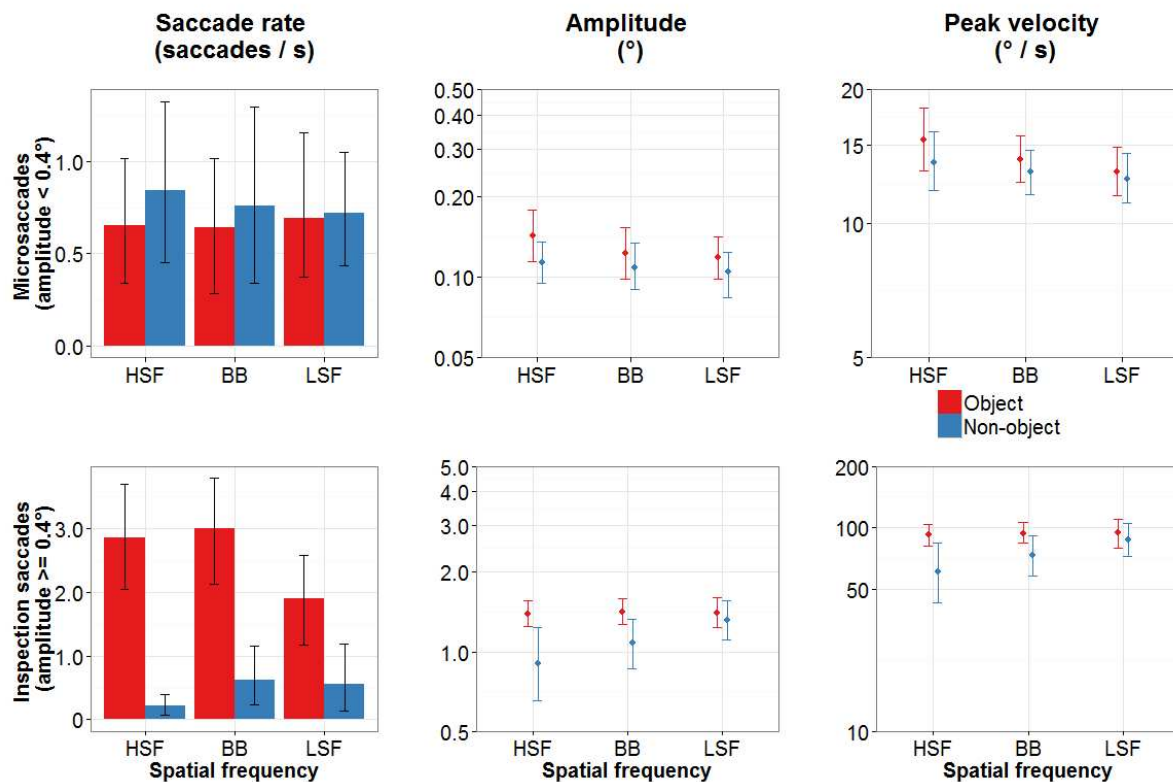
342 This graph shows the bimodal lognormal distribution of saccade amplitudes in the
 343 relevant time window (amplitudes are on a logarithmic scale). The reddish bars reflect
 344 the object conditions, the blueish bars the non-object conditions. The black line shows
 345 the average across conditions and, thus, reflects the time window 200-400 ms from
 346 Figure 3

347

348 We analyzed saccade rates, saccade amplitudes, saccade latencies and peak velocity
 349 of saccades in the time window 200-400 ms after stimulus onset (Figure 5) using repeated
 350 measures ANOVA with the factors Object and Spatial Frequency. In the analysis of
 351 amplitudes and peak velocity, subjects were excluded when they made no saccades in one of
 352 the conditions in the relevant time window. Thus, three subjects were excluded from the
 353 analysis of small microsaccades and five subjects in the analysis of large microsaccades. In
 354 the analysis of saccade rate, all subjects were included. 95% confidence intervals for the plots
 355 in Figure 5 were estimated using bootstrapping to generate surrogate distributions (1000

356 iterations) of mean saccade rate, amplitude, and velocity for each condition, as implemented
 357 in the ggplot2 package (Wickham, 2009) for R (R Core Team, 2015).

358



359

360 **Figure 5** Saccade characteristics separated for the two saccade types in the window
 361 from 200-400 ms after stimulus onset for objects (red) and non-objects (blue). The
 362 upper row shows microsaccades smaller than 0.4°, the lower row microsaccades of 0.4°
 363 and larger. The columns represent different saccade characteristics. Left column shows
 364 the saccade rate (N = 12; both rows), the centre column amplitudes (N = 9 upper row,
 365 N = 7 lower row), and right column peak velocity (N = 9 upper row, N = 7 lower row).
 366 Amplitude and peak velocity are plotted on a log scale. Error bars show bootstrapped
 367 95% confidence intervals, as described in the method. HSF - high spatial frequency, BB
 368 - broadband, and LSF - low spatial frequency images

369

370 **3.2.1 Small microsaccades (amplitude < 0.4°).** The analysis of saccade rates revealed
 371 no significant effects or interactions [Object: $F(1, 11) = 3.92$, $p = .07$, $\eta_g^2 = .01$; Frequency:
 372 $F(2, 22) < 1$; Object x Frequency: $F(2, 22) < 1$]. The same was true also for amplitudes
 373 [Object: $F(1, 8) = 4.69$, $p = .06$, $\eta_g^2 = .07$; Frequency: $F(2, 16) = 1.62$, $p = .23$, $\eta_g^2 = .02$; Object
 374 x Frequency: $F(2, 16) = 1.36$, $p = .28$, $\eta_g^2 = .02$] and latencies (Object: $F(1,9) = 0.10$, $p=0.75$,
 375 $\eta_g^2 = .002$; Frequency: $F(2,18) = 0.14$, $p = .87$, $\eta_g^2 = .004$; Object x Frequency: $F(2,18) = 0.86$,
 376 $p = 0.44$, $\eta_g^2 = 0.02$). The analysis of peak velocity showed a significant effect of Object, with
 377 significantly faster saccades in response to objects than to non-objects [$F(1, 8) = 6.99$, $p <$
 378 $.05$, $\eta_g^2 = .06$]. However, no other effects reached significance [Frequency: $F(2, 16) = 3.41$, p
 379 $= .06$, $\eta_g^2 = .05$; Object x Frequency: $F(2, 16) = 2.02$, $p = .17$, $\eta_g^2 = .01$].

380 **3.2.2 Large microsaccades (amplitude $\geq 0.4^\circ$).** The analysis of saccade rate revealed
 381 significant main effects of Object [$F(1, 11) = 37.53$, $p < .001$, $\eta_g^2 = .46$] and of Frequency
 382 [$F(2, 22) = 12.44$, $p < .001$, $\eta_g^2 = .04$] as well as a significant interaction of Object and
 383 Frequency [$F(2, 22) = 16.54$, $p < .001$, $\eta_g^2 = .05$]. Subsequent t-tests (p-value adjusted)
 384 revealed for all Frequency conditions higher saccade rates for objects compared with non-
 385 objects [BB: $t(11) = 6.28$, $p < .001$; HSF: $t(11) = 6.09$, $p < .001$; LSF: $t(11) = 4.58$, $p < .01$].
 386 While the different non-object conditions did not differ [BB vs. HSF: $t(11) = 1.98$, $p > .29$
 387 BB vs. LSF: $t(11) < 1$; HSF vs. LSF: $t(11) = 1.45$, $p = .53$], we found differences between
 388 object conditions. The saccade rate for HSF objects as well as for BB objects was higher
 389 compared with LSF objects [HSF vs. LSF: $t(11) = 6.61$, $p < .001$; BB vs. LSF: $t(11) = 7.18$, p
 390 $< .001$], whereas HSF objects and BB objects did not differ [$t(11) = 1.38$, $p = .53$].

391 Overall, the number of large microsaccades to non-objects was very low. Five out of
 392 the 12 participants did not show any saccade in one of the spatial frequency conditions.
 393 Therefore, we refrain from analyzing amplitudes, latencies and peak velocity for non-object
 394 conditions. For the analysis of object conditions, we found no significant effects of

395 Frequency in the analyses of amplitudes and peak velocity [$F_s < 1$]. However, we do find a
396 significant effect of Frequency in the analysis of latencies ($F(2,22) = 21.46$, $p < 0.001$, $\eta_g^2 =$
397 $.31$). Subsequent t-tests (p-value adjusted) reveal that latencies from all three conditions are
398 significantly different from each other, with BB objects eliciting the fastest saccades ($M =$
399 292ms , $SD=21\text{ms}$), followed by HSF objects ($M=312\text{ms}$, $SD=29\text{ms}$), with slowest saccades
400 for LSF objects ($M=335\text{ms}$, $SD=29\text{ms}$; BB vs. HSF: $t(11)=4.13$, $p = .003$; BB vs. LSF:
401 $t(11)=5.81$, $p<.001$; HSF vs. LSF: $t(11)=3.18$, $p=.009$).

402

403

4. Discussion

404 We investigated modulations of microsaccades during an object categorization task in which
405 objects or non-objects were presented with different scales of spatial frequency content. The
406 images were either unfiltered, broadband images, or filtered to contain only HSF or LSF
407 information. This allowed us to examine both high-level factors (i.e. the presence or absence
408 of an object) and low-level factors (i.e. spatial frequency content) simultaneously. We
409 observed the typical decrease and subsequent increase in saccade rate after visual stimulus
410 presentation (e.g., Engbert & Kliegl, 2003). Most relevant in the context of our study was the
411 clear peak in saccade rate in the time window 200 to 400 ms after stimulus onset. The size
412 and presence of this peak was modulated by the experimental manipulations. Specifically, the
413 peak rate was higher on object than non-object trials, as predicted on the basis of previous
414 work, and was higher for HSF and BB objects than for LSF objects.

415 Detailed analysis of the eye-tracking data revealed a bimodal distribution of the
416 amplitudes of saccades in response to the stimuli, suggesting two different classes of saccade:
417 small microsaccades with amplitudes below 0.4° , and large microsaccades with amplitudes
418 above 0.4° (Mergenthaler & Engbert, 2010). While it is tempting to suggest that small and
419 large microsaccades are generated by different underlying mechanisms, Otero-Millan et al.

420 (2013) argued that microsaccades and saccades fall on the same functional continuum, and
421 found that saccade rates across that continuum increase as stimulus size increases. Otero-
422 Millan et al. used a free-viewing paradigm in which all saccades over a 30-s trial are
423 considered. These saccades showed a unimodal amplitude distribution with a peak depending
424 on the stimulus size. In contrast, our results reflect the initial burst of saccades 200-400 ms
425 after stimulus onset during a brief stimulus presentation of 500 ms. Small microsaccades in
426 our study show the same characteristics (amplitude and peak velocity) as observed for
427 fixational events in Otero-Millan et al.'s study; our participants were asked to fixate a
428 fixation cross before and after stimulus exposure. Large microsaccades in our study show
429 similar amplitude and peak velocity as those in response to objects of comparable visual size
430 (~ 4 to 8°). Thus, the bimodal distribution we observe may reflect the sum of trials in which
431 the eyes remain fixated and trials in which the stimuli are inspected during this time window,
432 and thus may reflect both the demands of the task and the size of our stimuli, rather than
433 different classes of eye movement.

434 Otero-Millan et al. (2011) also found that microsaccades larger than 0.5° tended to
435 generate a corrective microsaccade, resulting in a square wave jerk. Corrective saccades may
436 be particularly likely with our object stimuli, given that participants are required to
437 discriminate between different categories, and must therefore inspect informative image
438 regions closely. Nevertheless, we found that our experimental manipulations had very little
439 effect on small microsaccades: there were no substantial effects of object or of spatial
440 frequency observed in the microsaccade rate, amplitude, or peak velocity. In contrast, the
441 large microsaccades were significantly affected by both the presence of an object and by the
442 spatial frequency content of the stimulus. Specifically, for large microsaccades, there were
443 higher saccade rates for objects than for non-objects. Furthermore, there were higher saccade
444 rates for HSF and BB objects than for LSF objects. For non-objects, there were no

445 differences in rate across different spatial frequencies. This suggests that when objects are
446 presented, more goal-directed inspection saccades may have been necessary to resolve the
447 spatial frequency information supporting object recognition. LSF objects also elicited slower
448 microsaccades than BB or HSF objects, but BB objects elicited even faster microsaccades
449 than HSF objects, indicating the importance of joining low and high spatial frequency
450 information for efficient guidance of eye movements. We suggest that this is consistent with
451 a first-pass, feedforward sweep determining if and where closer inspection was necessary,
452 with feedback mechanisms guiding small eye movements in resolving fine spatial detail (Ko
453 et al., 2010; Poletti, Listorti, & Rucci, 2013). Our findings are also consistent with McCamy
454 et al.'s (2014) finding that more microsaccades are directed to highly informative image
455 regions.

456 One additional possibility is that the additional task required for objects –
457 discrimination between living and non-living objects – may in part be responsible for
458 increasing the rate of larger microsaccades. We previously reported an increased rate of
459 microsaccades for objects versus non-objects in a task with a very different set of object and
460 non-object stimuli (Kosilo et al., 2013). No additional task beyond discriminating between
461 objects and non-objects was required in our previous study, suggesting that it is unlikely that
462 the additional task performed on objects here would explain all of the difference in
463 microsaccade rate between objects and non-objects. An account that combines bottom-up,
464 stimulus-driven effects with top-down task requirements is a more likely explanation.

465 Given the timing of our effects – 200 to 400 ms after stimulus onset – one might ask
466 to what extent these saccades contribute to correct object categorization. Previous studies
467 suggested that reasonably accurate broad categorization of objects is possible even with
468 exposure durations of around 100 ms or less (Thorpe et al., 1996; VanRullen & Thorpe,
469 2001). However, participants are often not able to identify the target objects correctly beyond

470 the initial broad categorization (see Evans & Treisman, 2005). These earlier studies often
471 used clear circumscribed categories as animal or vehicle sharing specific features (e.g., most
472 animals have legs) that can be used by the participants to categorize the target object without
473 identification. In addition, these target objects were often embedded in scenes that provided
474 further information on the gist of the scene. Moreover, categorization performance in our task
475 is much higher compared to the previous studies, at least in object conditions containing HSF
476 information (around 2.1% errors in HSF and BB object condition). While previous studies
477 suggested that LSF information is more relevant for object categorization with limited
478 exposure duration (Kihara & Takeda, 2010, 2012), our study clearly demonstrates that HSF
479 information contributes to enhance categorization performance (cf. the error rate of 16.6% in
480 the LSF object condition). The advantage of HSF information was not only found in error
481 rates but also RTs were much faster in the HSF and BB object condition compared with LSF
482 condition. Nevertheless, the categorization responses on objects took more than 700 ms on
483 average, and even the fastest response for a correct object categorization took more than 400
484 ms. In summary, saccades in this time window might well be supporting object identification
485 in our categorization task.

486 Note that in a previous report, we found that microsaccades were moderated by high-
487 level and low-level stimulus properties independently (Kosilo et al., 2013). Kosilo et al.'s
488 (2013) experiment required participants to discriminate between line drawings of objects and
489 non-objects that were closely matched to them in terms of various visual attributes, whilst
490 this study used noise texture patches as non-objects. The linear, high-frequency content of
491 non-objects in Kosilo et al. (2013) could have led to more microsaccades in the non-object
492 condition. Also, the specific low-level property which was manipulated differed across
493 studies (spatial frequency here; chromoluminance content there), so it is possible that high-
494 level/low-level interactions depend on the stimulus property which is manipulated.

495 The bimodal distribution of saccades in the present study has also important
496 methodical implications. When considering that differences between conditions in the present
497 study were only found for large microsaccades but not for small microsaccades, averaging
498 across all saccades can lead to invalid conclusions. Larger saccades are accompanied by
499 larger amplitudes and larger peak velocities. Thus, by averaging across all saccades, the
500 difference in the saccade rate of the inspection saccades would result in differences of the
501 mean amplitude and the mean peak velocity as well. However, these differences do not
502 reflect that larger or faster saccades were produced in a specific condition. Rather, it reflects
503 that overall more of the larger and faster saccades were produced. Some previous studies
504 reporting effects of cognitive factors on microsaccades subsume saccades with amplitudes up
505 to 1.5° or 2.0° (e.g. Engbert & Kliegl, 2003; Turatto et al., 2007; Yuval-Greenberg et al.,
506 2008), although other studies have already considered a detailed analysis of saccade size in
507 relationship to various stimulus properties (e.g. McCamy et al., 2012; Otero-Millan et al.,
508 2008; Troncoso et al., 2015). Given our finding, future research should take a closer look at
509 attributes of saccades elicited in their experiments and if they are found to fall within discrete
510 parts of the saccade continuum, they should be analysed separately. This will help to further
511 determine the functional role of microsaccades.

512 The findings of our study also bear methodological relevance for researchers wishing
513 to examine the induced gamma band signal using EEG, which is highly susceptible to
514 artefacts related to such eye movements. Although previous examinations of microsaccades
515 in comparable paradigms to those used in EEG have suggested that not all patterns of induced
516 gamma-band activity mirror those found in eye movements (Makin et al., 2011), we would
517 nevertheless suggest caution when the microsaccade rate cannot be directly examined via
518 eye-tracking or detection of miniature eye movements from eye channels (Craddock,
519 Martinovic, & Müller, 2016). A task that requires discrimination of complex stimuli is likely

520 to lead to large microsaccades even in the presence of the fixation cross (Kosilo et al., 2013).
521 Our study indicates that these eye movements reflect both low-level and high-level properties
522 of the stimulus in a way which is consistent with their role in sustaining efficient recognition
523 by guiding the acquisition of task-relevant information. Thus, any study of induced GBA that
524 does not account for microsaccadic artefact is likely to be confounding a range of bottom-up
525 and top-down effects that may be ocular or neural in origin.

526 In summary, the implications of our findings are clear: small saccadic eye movements
527 may be influenced by a combination of both high and low-level factors, and thus researchers
528 must be aware of this when manipulating such factors simultaneously. The finding that
529 spatial frequency content of images is differently utilised when categorising objects, as
530 opposed to distinguishing them from noise texture patches, fits well within the tenets of
531 object recognition models that posit a special role for low-level, spatial frequency
532 information content (e.g. Bar et al., 2006; Bullier, 2001; Hegdé, 2008; Sowden & Schyns,
533 2006). Furthermore, our study demonstrates that depending on the attributes of the stimuli
534 and the task, different manifestations of saccades may be observed. These different types of
535 saccades may come from discrete parts of the saccade continuum - in our study, as in
536 Mergenthaler and Engbert (2010), we observed both small and large (i.e., $> 1^\circ$)
537 microsaccades. Although small microsaccades were not modulated by low or high-level
538 factors, large microsaccades were, shedding further light on the strategic role of eye
539 movements in sampling the visual environment in order to acquire task-relevant information -
540 in this case, fine spatial detail that is indicative of object identity.

541 **Acknowledgements**

542 The project was funded by the Deutsche Forschungsgemeinschaft (DFG, MU 972/16-1). The
543 funders had no role in the design, collection, analysis and interpretation of data, in the writing
544 of the manuscript, or in the decision to submit the manuscript for publication.

545

546 **References**

- 547 Bar, M., Kassam, K. S., Ghuman, A. S., Boshyan, J., Schmid, A. M., Dale, A. M., ... Halgren, E. (2006).
548 Top-down facilitation of visual recognition. *Proceedings of the National Academy of Sciences*,
549 *103*(2), 449–454. <http://doi.org/10.1073/pnas.0507062103>
- 550 Bonneh, Y. S., Adini, Y., & Polat, U. (2015). Contrast sensitivity revealed by microsaccades. *Journal of*
551 *Vision*, *15*(9), 11–11.
- 552 Bosman, C. A., Womelsdorf, T., Desimone, R., & Fries, P. (2009). A Microsaccadic Rhythm Modulates
553 Gamma-Band Synchronization and Behavior. *The Journal of Neuroscience*, *29*(30), 9471 –
554 9480. <http://doi.org/10.1523/JNEUROSCI.1193-09.2009>
- 555 Bullier, J. (2001). Integrated model of visual processing. *Brain Research Reviews*, *36*(2-3), 96–107.
556 [http://doi.org/10.1016/S0165-0173\(01\)00085-6](http://doi.org/10.1016/S0165-0173(01)00085-6)
- 557 Craddock, M., Martinovic, J., & Müller, M. M. (2016). Accounting for microsaccadic artifacts in the
558 EEG using independent component analysis and beamforming. *Psychophysiology*, *53*(4),
559 553–565. <http://doi.org/10.1111/psyp.12593>
- 560 Di Lollo, V., Enns, J. T., & Rensink, R. A. (2000). Competition for consciousness among visual events:
561 The psychophysics of reentrant visual processes. *Journal of Experimental Psychology:*
562 *General*, *129*(4), 481–507. <http://doi.org/10.1037/0096-3445.129.4.481>
- 563 Dimigen, O., Valsecchi, M., Sommer, W., & Kliegl, R. (2009). Human Microsaccade-Related Visual
564 Brain Responses. *The Journal of Neuroscience*, *29*(39), 12321 –12331.
565 <http://doi.org/10.1523/JNEUROSCI.0911-09.2009>
- 566 Engbert, R. (2006). Microsaccades: a microcosm for research on oculomotor control, attention, and
567 visual perception. In S. L. M. S. Martinez-Conde (Ed.), *Progress in Brain Research* (Vol.
568 Volume 154, Part A, pp. 177–192). Elsevier. Retrieved from
569 <http://www.sciencedirect.com/science/article/pii/S0079612306540099>
- 570 Engbert, R., & Kliegl, R. (2003). Microsaccades uncover the orientation of covert attention. *Vision*
571 *Research*, *43*(9), 1035–1045. [http://doi.org/10.1016/S0042-6989\(03\)00084-1](http://doi.org/10.1016/S0042-6989(03)00084-1)

- 572 Evans, K. K., & Treisman, A. (2005). Perception of Objects in Natural Scenes: Is It Really Attention
573 Free? *Journal of Experimental Psychology: Human Perception and Performance*, *31*(6), 1476–
574 1492. <http://doi.org/10.1037/0096-1523.31.6.1476>
- 575 Fabre-Thorpe, M., Richard, G., & Thorpe, S. J. (1998). Rapid categorization of natural images by
576 rhesus monkeys. *Neuroreport*, *9*(2), 303–308.
- 577 Fintzi, A. R., & Mahon, B. Z. (2013). A Bimodal Tuning Curve for Spatial Frequency Across Left and
578 Right Human Orbital Frontal Cortex During Object Recognition. *Cerebral Cortex*.
579 <http://doi.org/10.1093/cercor/bhs419>
- 580 Goffaux, V., Peters, J., Haubrechts, J., Schiltz, C., Jansma, B., & Goebel, R. (2010). From Coarse to
581 Fine? Spatial and Temporal Dynamics of Cortical Face Processing. *Cerebral Cortex*.
582 <http://doi.org/10.1093/cercor/bhq112>
- 583 Hassler, U., Barreto, N. T., & Gruber, T. (2011). Induced gamma band responses in human EEG after
584 the control of miniature saccadic artifacts. *NeuroImage*, *57*(54), 1411–1421.
585 <http://doi.org/10.1016/j.neuroimage.2011.05.062>
- 586 Hegdé, J. (2008). Time course of visual perception: Coarse-to-fine processing and beyond. *Progress in*
587 *Neurobiology*, *84*(4), 405–439. <http://doi.org/10.1016/j.pneurobio.2007.09.001>
- 588 Hochstein, S., & Ahissar, M. (2002). View from the Top. *Neuron*, *36*(5), 791–804.
589 [http://doi.org/10.1016/S0896-6273\(02\)01091-7](http://doi.org/10.1016/S0896-6273(02)01091-7)
- 590 Kauffmann, L., Ramanoel, S., & Peyrin, C. (2014). The neural bases of spatial frequency processing
591 during scene perception. *Frontiers in Integrative Neuroscience*, *8*.
592 <http://doi.org/10.3389/fnint.2014.00037>
- 593 Keren, A. S., Yuval-Greenberg, S., & Deouell, L. Y. (2010). Saccadic spike potentials in gamma-band
594 EEG: Characterization, detection and suppression. *NeuroImage*, *49*(3), 2248–2263.
595 <http://doi.org/10.1016/j.neuroimage.2009.10.057>

- 596 Kihara, K., & Takeda, Y. (2010). Time course of the integration of spatial frequency-based
597 information in natural scenes. *Vision Research*, *50*(21), 2158–2162.
598 <http://doi.org/10.1016/j.visres.2010.08.012>
- 599 Kihara, K., & Takeda, Y. (2012). Attention-free integration of spatial frequency-based information in
600 natural scenes. *Vision Research*, *65*, 38–44. <http://doi.org/10.1016/j.visres.2012.06.008>
- 601 Ko, H., Poletti, M., & Rucci, M. (2010). Microsaccades precisely relocate gaze in a high visual acuity
602 task. *Nature Neuroscience*, *13*(12), 1549–1553. <http://doi.org/10.1038/nn.2663>
- 603 Kosilo, M., Wuerger, S. M., Craddock, M., Jennings, B. J., Hunt, A. R., & Martinovic, J. (2013). Low-
604 level and high-level modulations of fixational saccades and high frequency oscillatory brain
605 activity in a visual object classification task. *Perception Science*, *4*, 948.
606 <http://doi.org/10.3389/fpsyg.2013.00948>
- 607 Levin, D. T., Takarae, Y., Miner, A. G., & Keil, F. (2001). Efficient visual search by category: Specifying
608 the features that mark the difference between artifacts and animals in preattentive vision.
609 *Perception & Psychophysics*, *63*(4), 676–697. <http://doi.org/10.3758/BF03194429>
- 610 Li, F. F., VanRullen, R., Koch, C., & Perona, P. (2002). Rapid natural scene categorization in the near
611 absence of attention. *Proceedings of the National Academy of Sciences*, *99*(14), 9596–9601.
612 <http://doi.org/10.1073/pnas.092277599>
- 613 Makin, A. D. J., Ackerley, R., Wild, K., Poliakoff, E., Gowen, E., & El-Deredy, W. (2011). Coherent
614 illusory contours reduce microsaccade frequency. *Neuropsychologia*, *49*(9), 2798–2801.
615 <http://doi.org/10.1016/j.neuropsychologia.2011.06.001>
- 616 Martinez-Conde, S., Macknik, S. L., & Hubel, D. H. (2000). Microsaccadic eye movements and firing of
617 single cells in the striate cortex of macaque monkeys. *Nature Neuroscience*, *3*(3), 251–258.
618 <http://doi.org/10.1038/72961>
- 619 Martinez-Conde, S., Macknik, S. L., & Hubel, D. H. (2002). The function of bursts of spikes during
620 visual fixation in the awake primate lateral geniculate nucleus and primary visual cortex.

- 621 *Proceedings of the National Academy of Sciences*, 99(21), 13920–13925.
622 <http://doi.org/10.1073/pnas.212500599>
- 623 Martinez-Conde, S., Macknik, S. L., Troncoso, X. G., & Dyar, T. A. (2006). Microsaccades Counteract
624 Visual Fading during Fixation. *Neuron*, 49(2), 297–305.
625 <http://doi.org/10.1016/j.neuron.2005.11.033>
- 626 Martinez-Conde, S., Macknik, S. L., Troncoso, X. G., & Hubel, D. H. (2009). Microsaccades: a
627 neurophysiological analysis. *Trends in Neurosciences*, 32(9), 463–475.
628 <http://doi.org/16/j.tins.2009.05.006>
- 629 Martinez-Conde, S., Otero-Millan, J., & Macknik, S. L. (2013). The impact of microsaccades on vision:
630 towards a unified theory of saccadic function. *Nature Reviews Neuroscience*, 14(2), 83–96.
631 <http://doi.org/10.1038/nrn3405>
- 632 Martinovic, J., Gruber, T., & Müller, M. M. (2007). Induced Gamma Band Responses Predict
633 Recognition Delays during Object Identification. *Journal of Cognitive Neuroscience*, 19(6),
634 921–934. <http://doi.org/10.1162/jocn.2007.19.6.921>
- 635 Martinovic, J., Gruber, T., & Müller, M. M. (2008). Coding of Visual Object Features and Feature
636 Conjunctions in the Human Brain. *PLoS ONE*, 3(11), e3781.
637 <http://doi.org/10.1371/journal.pone.0003781>
- 638 Martinovic, J., Gruber, T., Ohla, K., & Müller, M. M. (2009). Induced Gamma-band Activity Elicited by
639 Visual Representation of Unattended Objects. *Journal of Cognitive Neuroscience*, 21(1), 42–
640 57. <http://doi.org/10.1162/jocn.2009.21004>
- 641 McCamy, M. B., Najafian Jazi, A., Otero-Millan, J., Macknik, S. L., & Martinez-Conde, S. (2013). The
642 effects of fixation target size and luminance on microsaccades and square-wave jerks. *PeerJ*,
643 1, e9. <http://doi.org/10.7717/peerj.9>
- 644 McCamy, M. B., Otero-Millan, J., Macknik, S. L., Yang, Y., Troncoso, X. G., Baer, S. M., ... Martinez-
645 Conde, S. (2012). Microsaccadic Efficacy and Contribution to Foveal and Peripheral Vision.

- 646 *The Journal of Neuroscience*, 32(27), 9194–9204. <http://doi.org/10.1523/JNEUROSCI.0515->
647 12.2012
- 648 McCamy, M. B., Otero-Millan, J., Stasi, L. L. D., Macknik, S. L., & Martinez-Conde, S. (2014). Highly
649 Informative Natural Scene Regions Increase Microsaccade Production during Visual
650 Scanning. *The Journal of Neuroscience*, 34(8), 2956–2966.
651 <http://doi.org/10.1523/JNEUROSCI.4448-13.2014>
- 652 Melloni, L., Schwiedrzik, C. M., Rodriguez, E., & Singer, W. (2009). (Micro)Saccades, corollary activity
653 and cortical oscillations. *Trends in Cognitive Sciences*, 13(6), 239–245.
654 <http://doi.org/16/j.tics.2009.03.007>
- 655 Mergenthaler, K., & Engbert, R. (2010). Microsaccades are different from saccades in scene
656 perception. *Experimental Brain Research*, 203(4), 753–757. <http://doi.org/10.1007/s00221->
657 010-2272-9
- 658 Oliva, A., & Schyns, P. G. (1997). Coarse Blobs or Fine Edges? Evidence That Information Diagnosticity
659 Changes the Perception of Complex Visual Stimuli. *Cognitive Psychology*, 34(1), 72–107.
660 <http://doi.org/10.1006/cogp.1997.0667>
- 661 Oliva, A., & Torralba, A. (2006). Chapter 2 Building the gist of a scene: the role of global image
662 features in recognition. In S. L. M. L. M. Martinez, J. -M. Alonso and P. U. Tse S. Martinez-
663 Conde (Ed.), *Progress in Brain Research* (Vol. 155, Part B, pp. 23–36). Elsevier. Retrieved from
664 <http://www.sciencedirect.com/science/article/pii/S0079612306550022>
- 665 Otero-Millan, J., Macknik, S. L., Langston, R. E., & Martinez-Conde, S. (2013). An oculomotor
666 continuum from exploration to fixation. *Proceedings of the National Academy of Sciences*,
667 110(15), 6175–6180. <http://doi.org/10.1073/pnas.1222715110>
- 668 Otero-Millan, J., Serra, A., Leigh, R. J., Troncoso, X. G., Macknik, S. L., & Martinez-Conde, S. (2011).
669 Distinctive Features of Saccadic Intrusions and Microsaccades in Progressive Supranuclear
670 Palsy. *The Journal of Neuroscience*, 31(12), 4379–4387.
671 <http://doi.org/10.1523/JNEUROSCI.2600-10.2011>

- 672 Otero-Millan, J., Troncoso, X. G., Macknik, S. L., Serrano-Pedraza, I., & Martinez-Conde, S. (2008).
673 Saccades and microsaccades during visual fixation, exploration, and search: Foundations for
674 a common saccadic generator. *Journal of Vision*, 8(14), 21. <http://doi.org/10.1167/8.14.21>
- 675 Peyrin, C., Michel, C. M., Schwartz, S., Thut, G., Seghier, M., Landis, T., ... Vuilleumier, P. (2010). The
676 Neural Substrates and Timing of Top-Down Processes during Coarse-to-Fine Categorization
677 of Visual Scenes: A Combined fMRI and ERP Study. *Journal of Cognitive Neuroscience*, 22(12),
678 2768–2780. <http://doi.org/10.1162/jocn.2010.21424>
- 679 Poletti, M., Listorti, C., & Rucci, M. (2013). Microscopic Eye Movements Compensate for
680 Nonhomogeneous Vision within the Fovea. *Current Biology*, 23(17), 1691–1695.
681 <http://doi.org/10.1016/j.cub.2013.07.007>
- 682 R Core Team. (2015). *R: A language and environment for statistical computing*. Vienna, Austria: R
683 Foundation for Statistical Computing. Retrieved from <http://www.r-project.org>
- 684 Rolfs, M. (2009). Microsaccades: Small steps on a long way. *Vision Research*, 49(20), 2415–2441.
685 <http://doi.org/10.1016/j.visres.2009.08.010>
- 686 Rousselet, G. A., Fabre-Thorpe, M., & Thorpe, S. J. (2002). Parallel processing in high-level
687 categorization of natural images. *Nature Neuroscience*, 5(7), 629–630.
688 <http://doi.org/10.1038/nn866>
- 689 Rucci, M. (2008). Fixational eye movements, natural image statistics, and fine spatial vision.
690 *Network: Computation in Neural Systems*, 19(4), 253–285.
691 <http://doi.org/10.1080/09548980802520992>
- 692 Rucci, M., Iovin, R., Poletti, M., & Santini, F. (2007). Miniature eye movements enhance fine spatial
693 detail. *Nature*, 447(7146), 852–855. <http://doi.org/10.1038/nature05866>
- 694 Siegenthaler, E., Costela, F. M., McCamy, M. B., Di Stasi, L. L., Otero-Millan, J., Sonderegger, A., ...
695 Martinez-Conde, S. (2014). Task difficulty in mental arithmetic affects microsaccadic rates
696 and magnitudes. *European Journal of Neuroscience*, 39(2), 287–294.
697 <http://doi.org/10.1111/ejn.12395>

- 698 Sowden, P. T., & Schyns, P. G. (2006). Channel surfing in the visual brain. *Trends in Cognitive*
699 *Sciences, 10*(12), 538–545. <http://doi.org/10.1016/j.tics.2006.10.007>
- 700 Tallon-Baudry, C., & Bertrand, O. (1999). Oscillatory gamma activity in humans and its role in object
701 representation. *Trends in Cognitive Sciences, 3*(4), 151–162. [http://doi.org/10.1016/S1364-](http://doi.org/10.1016/S1364-6613(99)01299-1)
702 [6613\(99\)01299-1](http://doi.org/10.1016/S1364-6613(99)01299-1)
- 703 Thorpe, S., Fize, D., & Marlot, C. (1996). Speed of processing in the human visual system. *Nature,*
704 *381*(6582), 520–522. <http://doi.org/10.1038/381520a0>
- 705 Thorpe, S., Gegenfurtner, K. R., Fabre-Thorpe, M., & Bülthoff, H. H. (2001). Detection of animals in
706 natural images using far peripheral vision. *European Journal of Neuroscience, 14*(5), 869–
707 876. <http://doi.org/10.1046/j.0953-816x.2001.01717.x>
- 708 Troncoso, X. G., McCamy, M. B., Jazi, A. N., Cui, J., Otero-Millan, J., Macknik, S. L., ... Martinez-Conde,
709 S. (2015). V1 neurons respond differently to object motion versus motion from eye
710 movements. *Nature Communications, 6*, 8114. <http://doi.org/10.1038/ncomms9114>
- 711 Turatto, M., Valsecchi, M., Tamè, L., & Betta, E. (2007). Microsaccades distinguish between global
712 and local visual processing: *NeuroReport, 18*(10), 1015–1018.
713 <http://doi.org/10.1097/WNR.0b013e32815b615b>
- 714 VanRullen, R. (2007). The power of the feed-forward sweep. *Advances in Cognitive Psychology, 3*(1),
715 167–176. <http://doi.org/10.2478/v10053-008-0022-3>
- 716 VanRullen, R., & Thorpe, S. J. (2001). The Time Course of Visual Processing: From Early Perception to
717 Decision-Making. *Journal of Cognitive Neuroscience, 13*(4), 454–461.
718 <http://doi.org/10.1162/08989290152001880>
- 719 Wickham, H. (2009). *ggplot2: Elegant Graphics for Data Analysis*. New York: Springer-Verlag.
- 720 Yuval-Greenberg, S., Tomer, O., Keren, A. S., Nelken, I., & Deouell, L. Y. (2008). Transient Induced
721 Gamma-Band Response in EEG as a Manifestation of Miniature Saccades. *Neuron, 58*(3),
722 429–441. <http://doi.org/10.1016/j.neuron.2008.03.027>
- 723